The $^{40}Ar/^{39}Ar$ dating of magmatic activity in the Donbas Fold Belt and the Scythian Platform (Eastern European Craton)

P. Alexandre,[1] F. Chalot-Prat,[2] A. Saintot,[3] J. Wijbrans,[3] R. Stephenson,[3] M. Wilson,[4] A. Kitchka,[5] and S. Stovba[6]

Received 12 September 2003; revised 15 April 2004; accepted 23 June 2004; published 4 September 2004.

[1] The Donbas Fold Belt is the compressionally deformed southeasternmost part of the intracratonic late Paleozoic Dniepr-Donets rift basin. It is situated in an intracratonic setting but close to the southern margin of the East European Craton, south of which lies the Scythian Platform. A range of igneous rocks from the Donbas Fold Belt and the Scythian Platform were dated by the $^{40}Ar/^{39}Ar$ method in order to constrain the ages of magmatic activity in these areas, and compare them. The plateau ages from the south margin of the Donbas Fold Belt vary from 151.4 ± 4.7 Ma to 278.1 ± 5.3 Ma, and define three main age groups: Middle-Late Jurassic, Middle-Late Triassic, and Early Permian. The age spectra obtained from the Scythian Platform samples are often disturbed as a result of limited alteration. The proposed ages (plateau and pseudoplateau) vary from 174.4 ± 2.1 Ma to 243.7 ± 1.4 Ma, and two major age groups are defined, in Early Carboniferous and Triassic/Jurassic times. The Early Permian (285–270 Ma) and Early Triassic (245–250 Ma) ages of magmatic activity are the same in both areas; in the Late Triassic, the ages of magmatic activity are slightly different (220 and 205 Ma), and they are entirely different thereafter. These data can be interpreted as indicating a mantle plume as common deep magmatic source. *INDEX TERMS:* 1035 Geochemistry: Geochronology; 8149 Tectonophysics: Planetary tectonics (5475); 8121 Tectonophysics: Dynamics, convection currents and mantle plumes; *KEYWORDS:* geochronology, $^{40}Ar/^{39}Ar$, Donbas Fold Belt, Scythian Platform, magmatic activity, mantle plume. **Citation:** Alexandre, P., F. Chalot-Prat, A. Saintot, J. Wijbrans, R. Stephenson, M. Wilson, A. Kitchka, and S. Stovba (2004), The $^{40}Ar/^{39}Ar$ dating of magmatic activity in the Donbas Fold Belt and the Scythian Platform (Eastern European Craton), *Tectonics*, *23*, TC5002, doi:10.1029/2003TC001582.

[1]Department of Geological Sciences, Queen's University, Kingston, Ontario, Canada.
[2]Centre de Recherches Pétrographiques et Géochiminiques, CNRS, Vandoeuvre-les-Nancy, France.
[3]Faculteit der Aard en Levenswetenschappen, Tektoniek afdeling, Vrije Universiteit, Amsterdam, Netherlands.
[4]School of Earth Sciences, University of Leeds, Leeds, UK.
[5]Centre for Aerospace Research for the Earth (CASRE), Kiev, Ukraine.
[6]Technology Centre, Kiev, Ukraine.

0278-7407/04/2003TC001582

1. Introduction

[2] The Donbas Fold Belt is part of a large late Paleozoic intracratonic rift basin transecting the Precambrian East European Craton, the Pripyat-Dniepr-Donets Basin (DDB) oriented WNW-ESE [*Stovba et al.*, 1996] (Figure 1). Sediment thicknesses increase from ~2 km in the Pripyat Trough to as much as 22 km in the Donbas Fold Belt [*Chekunov et al.*, 1993; *Stovba and Stephenson*, 1999; *Kusznir et al.*, 1996b]. The Donbas Fold Belt is the mildly deformed and inverted southeastern part of the rift basin. It is bordered on the southwest by the Priazov Massif (part of the Early Proterozoic Ukrainian Shield) and to the north by the Voronezh Massif (corresponding to the Ukrainian Shield) [*Shchipansky and Bogdanova*, 1996]. To the east it connects with the deformed southern margin of the Russian Platform (Karpinsky Swell). The Scythian Platform is situated to the south of the Ukrainian shield and the Donbas Fold Belt, and to the north of the Great Caucasus (Figure 1).

[3] There are very few absolute ages of magmatic activity in the region, particularly for the Donbas Fold Belt or the Scythian Platform. The strong magmatic activity that is associated with the initiation of the DDB rift is mostly Late Devonian, in a context of active rifting conditions [*Shatalov*, 1986]. Other stages of magmatism have been described during the Permian, the Triassic, and the Jurassic [*Shatalov*, 1986], in different contexts. A synthesis [*Shatalov*, 1986, and references therein] of the existing K-Ar ages of dikes from the Priazov Massif (south of Donbas; Figure 1) indicates the presence of episodes of magmatic activity with ages similar to those derived by the stratigraphy in the Donbas: 156 ± 11 Ma (n = 4), 223 ± 16 Ma (n = 38), 286 ± 11 Ma (n = 35), 340 ± 14 Ma (n = 17), and 388 ± 12 Ma (n = 10).

[4] As the magmatism has strong relevance to the development of the rift and its geodynamic evolution, the absolute ages of magmatic activity form an important piece of information permitting us to constrain the evolution of this part of the Eastern European Craton (EEC), and possibly providing information on the source(s) of the magmatism. Thus the main purpose of the present study was to constrain the ages of the magmatic (mostly volcanic) activity in the Donbas Fold Belt and the Scythian Platform,

and compare these with data from adjacent areas, and to propose interpretations in terms of the origin and timing of igneous activity. The method used is laser single-grain and whole rock $^{40}Ar/^{39}Ar$ dating of volcanic rocks, dikes, and veins from the southern part of the Donbas Fold Belt and from the Scythian Platform.

2. Geological Context

2.1. Scythian Platform

[5] The deeper part of the sedimentary cover of the Scythian Platform is not very well understood. The basement for these sediments is thought to be late Paleozoic (Hercynian?). According to *Nikishin et al.* [1996], the Scythian Platform has undergone several extensional tectonic events (rifting phases during the Devonian, Carboniferous/Permian boundary, and Permian/Triassic boundary), separated by intraplate compressional tectonics (Silurian to Early Devonian, Early to Middle Devonian, Middle Late Carboniferous, Early Permian, and Triassic/Jurassic boundary). Several phases of magmatism have been recorded, related to the extensional and compressional events affecting the Scythian Platform. Basaltic magmatism was predominant during an Early-Middle Triassic phase of active extension, related to back arc rifting [*Robinson*, 1997; *Nikishin et al.*, 2001]. During the Late Triassic, rifting was interrupted by a compressional event, which continued into the Early Jurassic. The main basin at this time, the Nogiask basin, was infilled with molasse and andesitic to rhyolitic volcanics.

2.2. Donbas Fold Belt

[6] The sediment thickness in the Donbas Fold Belt is greater than 20 km [*Stovba and Stephenson*, 1999; *Stovba et al.*, 2003]. Large coal deposits make it economically important; the fact that it represents the inverted part of the intracratonic Pripyat-Dniepr-Donets rift makes it of major importance for the study and understanding of the evolution of intracratonic sedimentary basins such as the DDB.

[7] Prior to the onset of crustal extension, the Priazov and Voronezh Massifs were covered by marine Middle Devonian sediments [*Stovba et al.*, 1996; *Alekseev et al.*, 1996]. During the Late Devonian, rifting was widespread from the Pripyat-Dniepr-Donets system in the south to the Barents Sea in the north [*Wilson and Lyashkevich*, 1996], locally associated with domal basement uplift and magmatism. The evolution of this rift system may be contemporaneous with the development of a major back arc rift system in western and central Europe [*Ziegler*, 1990].

[8] Rift development in the Pripyat-Dniepr-Donets region occurred in several stages [*Stephenson et al.*, 1993; *Stovba and Stephenson*, 1999; *Kusznir et al.*, 1996a]: there are two major phases of rifting (Late Devonian and Early Carboniferous) and extensional rejuvenation in Serpukhovian, (Middle Carboniferous), and in latest Carboniferous-Early Permian times associated with major uplift of the southern shoulder of the Donbas (the Priazov massif) [*Stovba and Stephenson*, 1999]. A postrift subsidence phase (Permian to Late Cretaceous) is interrupted by compressional tectonics during Triassic-Jurassic times. Major tectonic inversion of the Donbas (with thrust and fold development) occurred during the late Late Cretaceous [*Stovba and Stephenson*, 1999; *Saintot et al.*, 2003a, 2003b]. It was during the main extensional stage (Frasnian to Famennian, circa 370 to 355 Ma) that the maximum rates of subsidence occurred [*Kusznir et al.*, 1996a].

2.3. Magmatism in the Donbas Fold Belt

[9] All stages of rifting were accompanied by intense volcanic activity, probably mantle plume-related [*Wilson and Lyashkevich*, 1996]. Different studies [e.g., *Donskoy*, 1982; *Shatalov*, 1986; *McCann et al.*, 2003] describe several stages of magmatic activity in their tectonic contexts. The ages indicated by different authors are derived from stratigraphic relationships. The major stage of volcanic activity is related to the main rifting episodes (Late Devonian, 380–355 Ma) and is accompanied by the emplacement of large volumes of extrusive rocks (alkali basalts in a broad sense, dacites, rhyolites) and dikes (kimberlites, diabases). Three less important stages of magmatic activity occurred during the subsequent development of the basin: an Early Permian (290–270 Ma) shonkinite-monzonite-plagioporphyric complex occurring only in the south Donbas, and presumably related to extensional reactivation of the rift with strong uplift of the southern part of the Donbas; Early Triassic (230–200 Ma) andesites and trachyandesites (in the context of back arc extension); and Late Jurassic-Early Cretaceous (160–115 Ma) lamprophyres (monchiquites) and dolerites, occurring only on the south margin of the Donbas Fold Belt in the context of intraplate extension [*De Boorder et al.*, 1996].

3. Sampling

[10] The purpose of the sampling was to provide a representative set of the lithologies present in the respective areas. Only samples showing no or little signs of alteration were taken. The location of the samples is indicated on the maps (Figures 1 and 2) and on the synthetic logs (Figures 3 and 4). All samples studied are listed in Table 1, together with their locations and rock types. Two distinct areas were sampled: nine samples come from the south margin of the Donbas Fold Belt and six from the Scythian Platform.

3.1. South Margin of Donbas Fold Belt

[11] Three lithological groups were sampled here (Table 1): dacites (UK12, UK55, and 37-1), trachyandesites (UK06 and UK07), and basic rocks (N2, N4, 34-3, and UK39C). The sampled rocks are either extrusive (lava flows and domes) or intrusive (dikes and veins; Figure 4).

[12] The dacites crop out either as small lava domes (UK12), or subsurface metric to plurimetric dikes (37-1 and UK55). The dikes crosscut either basaltic flows (37-1) or the Priazov Proterozoic granitic basement (UK55). On the basis of field relationships and petrographic observations [*McCann et al.*, 2003], the dacitic domes were proposed to be interstratified within the Devonian sequence,

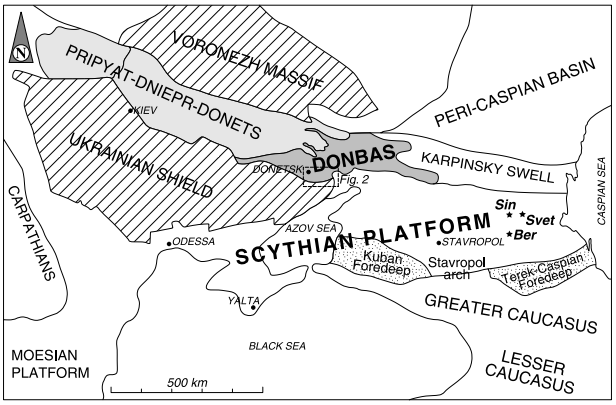

Figure 1. Simplified geological sketch map of the studied area, with the major geotectonic units indicated. The area covered in Figure 2 is indicated. The location of the drill holes in the Scythian Platform is indicated: Abbreviations are as follows: Sin, Sinebugrovskaya; Svet, Svetloiarskaya; Ber, Berezkinskaya.

between basaltic flows below and rhyolitic ignimbrites above (Figure 4). Only amphiboles from these dacitic samples were separated for dating (Table 1). For a detailed description, see *McCann et al.* [2003].

[13] The trachyandesites crop out either as flows and domes (UK06 and UK07), or subsurface metric to plurimetric dykes and sills. The dikes, not selected for dating because of strong alteration, are found crosscutting the Priazov Proterozoic granitic basement, the Devonian basaltic suite and the Tournaisian limestones (Figure 4) where sills are also numerous. From field relationships and petrographic observations [*McCann et al.*, 2003], the trachyandesitic lava flows or domes were assumed to be emplaced at the surface during a single magmatic event between the earliest Visean and late early Visean. Amphiboles from UK06 and UK07, and also plagioclase from UK06 were separated for dating (Table 1). For detailed description, see *McCann et al.* [2003].

[14] The basic rocks (basanites and tephrites and alkali gabbros) crop out as metric to plurimetric dikes or veins (34-3 and UK39C) forming subvertical networks at a plurikilometric scale in two distinct areas (Figure 2), or come from drill holes (N2 and N4). In both cases they crosscut Carboniferous sediments. The rocks are either partially crystalline (porphyritic microlitic with glassy patches) and vesiculated, or totally crystalline (finely to crudely granular). Their mineral assemblage includes euhedral phlogopite and/or brown amphibole in different proportions, euhedral olivine (sometimes with mantle olivine xenocrysts) and/or Ti-augite, euhedral magnetite, subhedral to anhedral plagio-

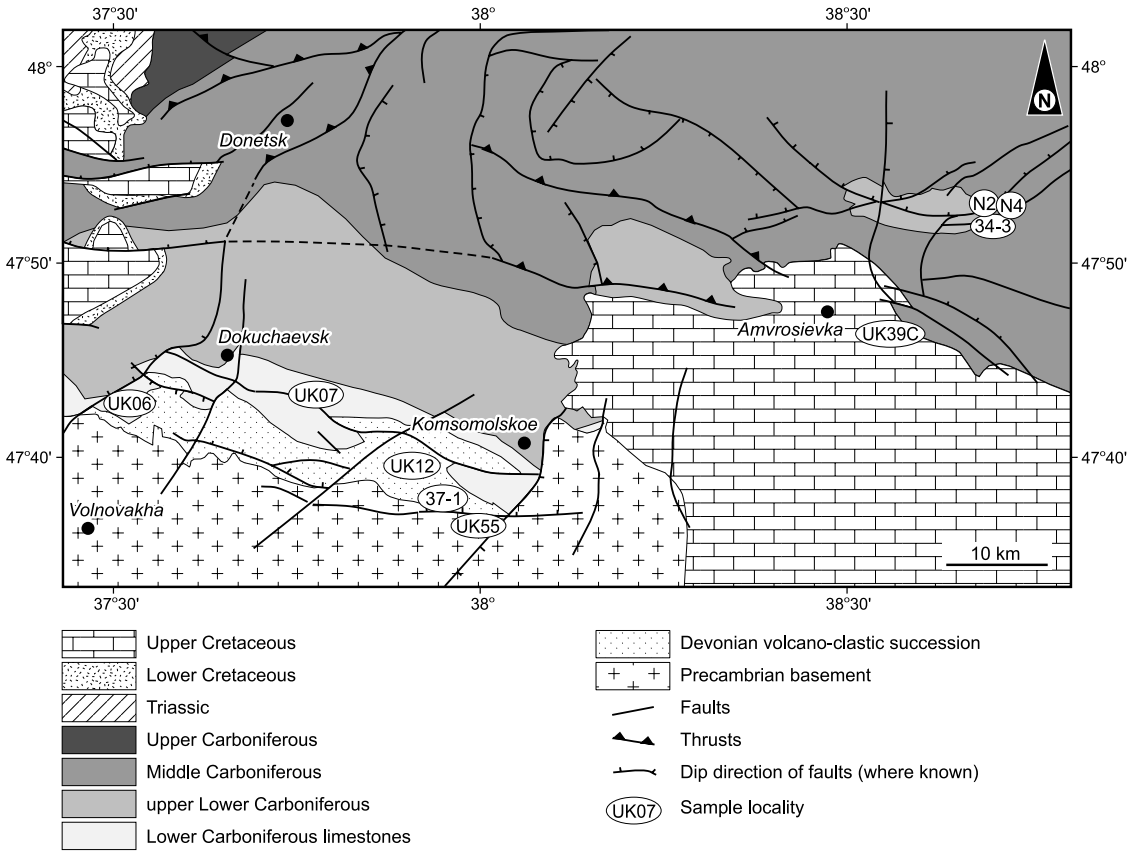

Figure 2. Simplified geological map of the southwestern margin of the Donbas Fold Belt, with the position of the dated samples indicated.

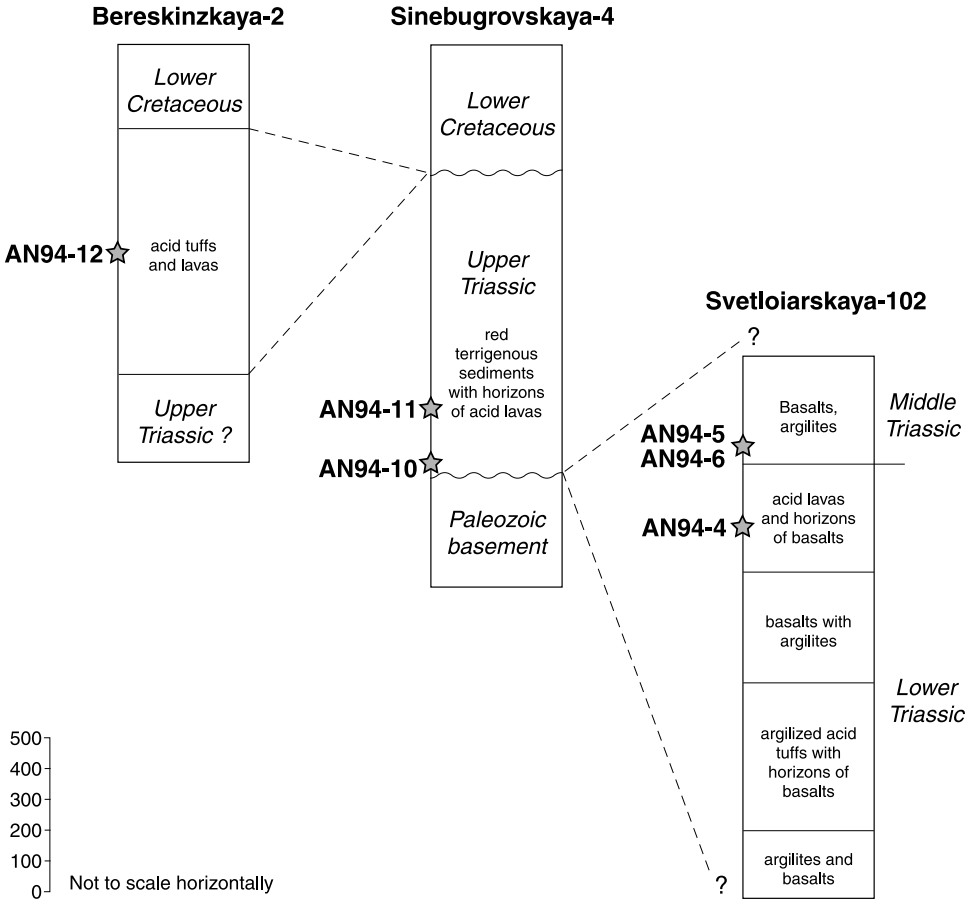

Figure 3. Simplified stratigraphic column as observed in the three boreholes in the Scythian Platform. The position of the dated samples is indicated.

clase, anhedral calcite and sometimes rare anhedral Mg-biotite. They belong to the same alkaline group and are assumed to have been emplaced during a post-Carboniferous magmatic event. Biotites (in basanites) or amphiboles (in gabbros) were separated for dating (Table 1).

3.2. Scythian Platform

[15] Volcanic samples (lava flows and tephras) were obtained from three drill holes penetrating the lowest parts of the sedimentary cover. The samples studied are (Figure 3 and Table 1) as follows: two basaltic lava flows from the Middle Triassic sequence (AN94-5 and AN94-6) and four acidic tephras from the Lower Triassic (AN94-4, rhyolite), the Upper Triassic (AN94-10, rhyolite, and AN94-11, dacite), and the Jurassic (?) (AN94-12, rhyolite) series.

4. Analytical Procedure

[16] The hand samples were crushed in a jaw crusher and sieved. In three samples (UK07, UK12, and UK39C) the minerals of interest were relatively small and, accordingly, the fine fraction (50–150 μm) was used (Figure 5). For all other samples, the 150–350 μm fraction was used. As two samples (UK05 and UK12, Figure 5) showed the presence of weak to moderate alteration, they were washed in 10% hydrofluoric acid (HF) for several seconds. All samples were washed in an ultrasonic bath and then rinsed several times in alcohol and then in deionized water. About 20 individual grains of the minerals of interest were hand picked under a binocular microscope and wrapped in aluminum foil. They were packed together with irradiation monitors (the GA1550 biotite standard with age of 98.8 Ma) [*Renne et al.*, 1998]; one monitor was placed between every five unknowns. The samples were irradiated for 24 hours in the Cd-shielded RODEO position of the HFR reactor in Petten, Netherlands. The variation of the irradiation over the length of the can was not significant, did not follow a specific trend, and was smaller than the variation for an individual monitor position. Therefore the average value of the J-value (0.006556 ± 0.000054, or ±0.82%) for the five monitors framing the samples for this study was taken for all of them.

[17] Extraction and analysis of argon was performed at the Vrije Universiteit (Amsterdam). The individual grains were heated using a defocused, continuous argon ion laser beam, for 1 min. The extraction was done by step heating (the number of steps was between 5 and 10, typically 7).

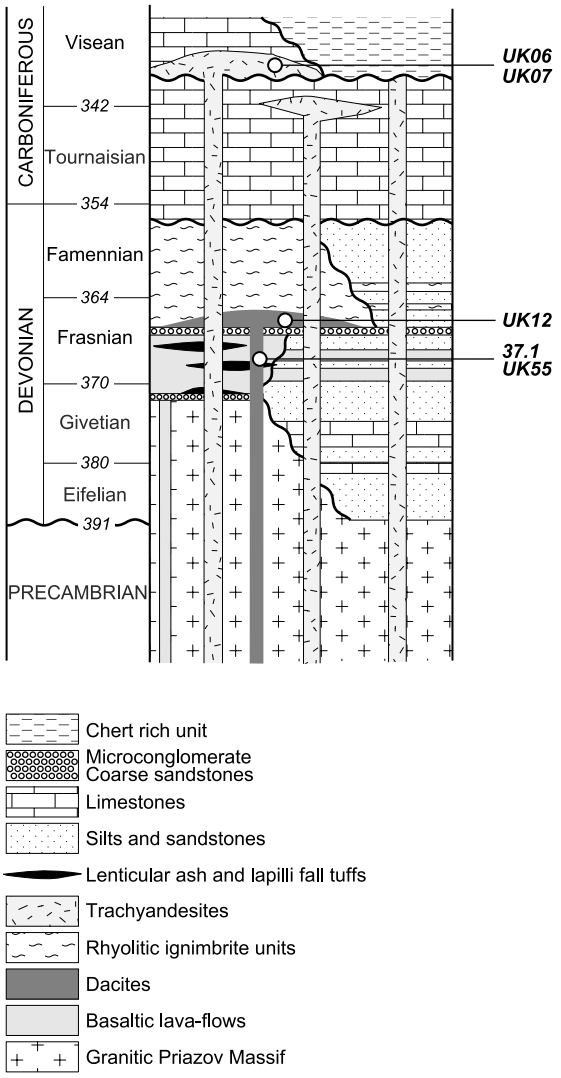

Figure 4. Simplified stratigraphic column for the south margin of the Donbas Fold Belt. The position of the dated samples is indicated. After *McCann et al.* [2003].

The extracted gases were purified using a Zr-Al SAES AP10GP getter (400°C) and a double Fe-V-Zr SAES St172 getter (250°C) for 5 min. The five argon isotopes and appropriate baselines at the half-mass limits were analyzed in a MAP 215-50 mass spectrometer in 10 cycles, in peak-jumping mode. Blank intensities were measured every 3 or 4 sample step runs. For the masses analyzed, the inlet intensities were calculated using exponential curves (masses 40 and 39) or linear regressions (masses 38, 37, and 36) using ArArCalc data reduction software [*Koppers*, 2002].

[18] The criteria defining a plateau age used in this work are the following: the plateau should represent at least three consecutive steps, corresponding to at least 70% of the total amount of $^{39}Ar_K$ released, the ages of the steps in the plateau should be concordant at the 1σ level. The calculated MSWD over the steps forming a plateau is usually <2.0. All isotopic measurements were corrected for K and Ca isotopic interferences, mass discrimination, and atmospheric argon contamination. All error margins quoted are in the 2σ confidence level.

5. Analytical Results

[19] Ten mineral separates from the southwest Donbas margin (three biotites, six amphiboles, and one plagioclase), and six whole rocks from the Scythian Platform were analyzed. All results are given in Table 2 and Figures 6 and 7.

5.1. Southwest Donbas Margin

[20] All ten mineral separates yielded plateau ages, within 80 % or more of the gases on the plateau (Figure 6). The 2σ uncertainty margins are typical for the method (between ±3.9 and ±14.2 Ma, typically ±5 Ma; Table 2). Two samples (UK07 and UK12) have significantly higher error margins (circa ± 30 Ma); this is explained by the low intensities obtained because of the small amount of potassium in the mineral analyzed (amphibole). The age spectra of four of the samples (UK39c, N2, $UK06_{plagioclase}$, and $UK06_{amphibole}$) have one step much larger than the others (49 to 66% of the total $^{39}Ar_K$ released). Nevertheless, this does not affect the validity of the calculated plateau ages, as the large step is, in every case, well concordant with the other steps on the plateau.

[21] The $^{40}Ar/^{39}Ar$ ages obtained from the samples in the southwest Donbas basin margin form three main age groups, with average ages of 277.9 ± 0.3 Ma (Early Permian; $UK06_{amphibole}$ and N4), 218.5 ± 5.5 Ma (Late Triassic; samples 37-1, UK55, UK07, and UK12), and 153.3 ± 2.0 Ma (Late Jurassic; samples N2, 34-3, and UK39c). One sample ($UK06_{plagioclase}$) has an age of 251.4 ± 4.2 Ma (Permian-Triassic boundary; Figure 6). The error margins on these averages correspond to the dispersion of the plateau ages, and do not take into account the errors on the individual plateau ages.

5.2. Scythian Platform

[22] The six analyses of whole rock samples provided disturbed age spectra (Figure 7). Only three pseudoplateau ages were defined, for samples AN94-4 (204.7 ± 2.1 Ma, defined on the basis of 63% of argon released), AN94-5 (192.9 ± 1.1 Ma, 34% of argon), and AN94-12 (174.4 ± 2.1 Ma, 42% of argon). For sample AN94-5, there is a relatively flat portion in the low-temperature steps, with an average age of circa 208 Ma (Figure 7). A similar shape is observed for sample AN94-6, where two relatively flat portions can be observed (at low-temperature steps and at high-temperature steps), without meeting the requirements for a plateau age, and for which average ages have been calculated: 193.9 ± 5.6 Ma and 178.7 ± 2.9 Ma. In this case, there are probably two different argon isotopic reservoirs in the sample, as the two portions of the spectrum correspond to two distinct ^{37}Ar contents indicating two distinct calcium concentrations. The same is probably valid for sample AN94-5 (same shape as sample AN94-6), and probably for sample AN94-12, where the high-temperature steps

Table 1. List of the Samples Analyzed From the Donbas Fold Belt and the Scythian Platform

Sample	Localization	Outcrop Type	Rock Type	Mineral Dated
		Donbas Fold Belt		
UK06	Novotroitskoe	lava flow	trachyandesite	plagioclase, amphibole
UK07	Sukha Volnovakha	lava flow	trachyandesite	amphibole
UK12	Styla Horst	lava flow	dacite	amphibole
UK55	Razdolnoe	dike	dacite	amphibole
37-1	Razdolnoe	dike	dacite	amphibole
N2	Artemovka	vein (in drill hole)	alkali gabbro	amphibole
34-3	Artemovka	vein	alkali monzonite	biotite
N4	Artemovka	dike (in drill hole)	tephrite	biotite
UK39C	Amvrosievka	dike	basanite	biotite
		Scythian Platform		
AN 94-4	Svetloiarskaya	tephra (in drill hole)	rhyolite	whole rock
AN 94-5	Svetloiarskaya	lava flow (in drill hole)	basalt	whole rock
AN 94-6	Svetloiarskaya	lava flow (in drill hole)	basalt	whole rock
AN 94-10	Sinebugrovskaya	tephra (in drill hole)	rhyolite	whole rock
AN 94-11	Sinebugrovskaya	tephra (in drill hole)	dacite	whole rock
AN 94-12	Bereskinzkaya	tephra (in drill hole)	rhyolite	whole rock

define an age of 205.4 ± 3.1 Ma (Figure 7). It is difficult to define an age for sample AN94-11, as one step has more than 50% of the released argon and the spectrum is quite irregular. Two high-temperature steps of this spectrum are concordant and their average age is circa 195 Ma. Finally, it is impossible to obtain any age information for sample AN94-10, where the spectrum is very disturbed (the integrated age is 243.5 ± 1.4 Ma).

[23] All the samples from the Scythian Platform have disturbed age spectra, which probably indicates the presence of different isotopic reservoirs, corresponding to different phases. This is possibly further complicated by thermal perturbations and/or alteration as observed under the microscope. Nevertheless, the pseudoplateau ages and the flat portion ages define age groups at circa 205 Ma (limit Triassic-Jurassic; sample AN94-4, high-temperature steps of sample AN94-12, low-temperature steps of sample AN94-5), circa 193-195 Ma (Early Jurassic; flat parts of the steps of samples AN94-5, AN94-6, and AN94-11), and circa 174–179 Ma (Middle Jurassic; flat portion of the spectrum for samples AN94-6 and pseudoplateau for sample AN94-12).

6. Discussion

6.1. Validity of the $^{40}Ar/^{39}Ar$ Ages

[24] All ten minerals from the Donbas Fold Belt provided plateau ages (Figure 6). As the corresponding rocks were in all cases emplaced in portions of the crust where the host rock temperature was lower than the closure temperature for the dated minerals (Table 1), the ages obtained correspond to the emplacement ages of the corresponding rock or to a complete reopening and resetting of their argon isotopic systems at a later time.

[25] For sample UK06, the plateau ages obtained on plagioclase and amphibole are different, respectively, circa 251 and circa 278 Ma. As the emplacement of the rock occurred at temperatures lower than the closure temperature for both minerals analyzed [*McDougall and Harrison*, 1999], differential cooling history cannot be invoked to explain the difference in age. A possible explanation is the effects of alteration (the plagioclase is altered, Figure 5), but one would expect to obtain a strongly irregular age spectrum instead of the perfect plateau age (Figure 6). Another possible explanation of the difference between the ages of plagioclase and amphibole in this sample is a thermal perturbation resulting in complete reopening of the argon isotopic system of the plagioclase at circa 251 Ma, without affecting the argon isotopic system of the amphibole. This thermal perturbation, arguably produced by the emplacement of a magmatic body in the near vicinity, would have increased the temperature of the trachyte (sample UK06) to well above 250°C (closure temperature for plagioclase) [*McDougall and Harrison*, 1999], and lower than ~550° to 650°C (closure temperature for amphibole) [*Villa*, 1998; *McDougall and Harrison*, 1999]. Thus it can be suggested that sample UK06 records two distinct ages of magmatic activity, the first being the age of initial emplacement of the unit, the second the age of a subsequent magmatic event. However, a reheating of the rock to a temperature higher than 250°C would be expected to produce visible modification of the dated rock, mainly recrystallizations, which is not observed.

[26] All whole rock age spectra from the Scythian Platform are disturbed (Figure 7), which hampers their interpretation. Nevertheless, it is possible to propose that the three age groups indicated above correspond to real ages, as they are reproducible in distinct samples, on pseudoplateaus or on flat portions of the spectrum (Figure 7).

6.2. Comparison of the Ages Obtained With the Stratigraphic Ages Derived From Field Observations

6.2.1. Donbas

[27] The basic igneous rocks were sampled either in near-surface intrusions (34-3 and UK39C) or in drill holes (N2 and N4), which precluded definition of stratigraphic age. Thus the $^{40}Ar/^{39}Ar$ ages obtained for these samples will be considered emplacement ages. These belong to two distinct age groups,

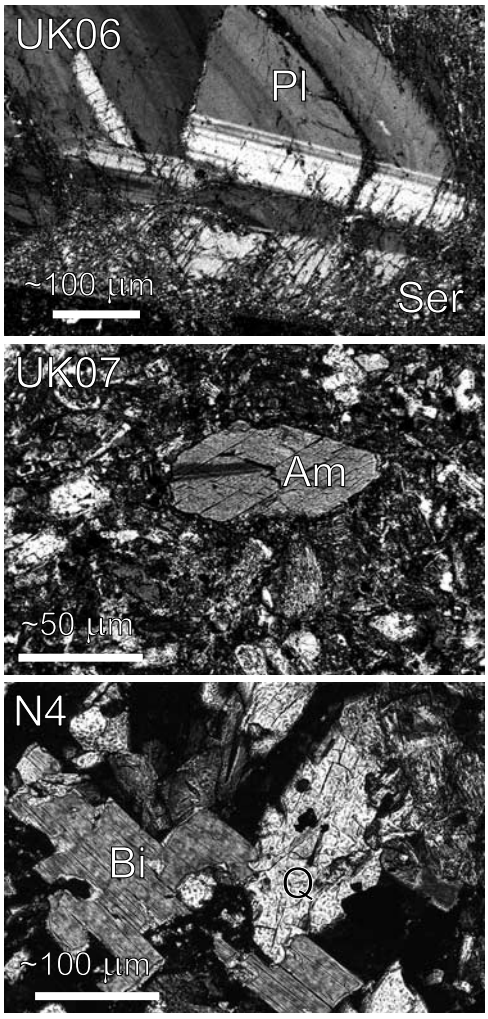

Figure 5. Photomicrographs of some of the dated minerals, in samples from the Donbas Fold Belt. Note (top) the sericitization of plagioclase in sample UK06, (middle) the small size of the amphibole in sample UK07, and (bottom) the limited alteration of biotite in sample N4.

at circa 153 Ma (Late Jurassic; N2, 34-3, and UK39C) and at circa 278 Ma (Early Permian; N4; Figure 6). This was somewhat unexpected given that the mineralogy and geochemistry of these rocks are very similar; they differ only in texture.

[28] The chronostratigraphic age of the two trachyandesitic samples (UK06 and UK07) was defined as early Visean (circa 340 Ma; Figure 4) on the basis of the assumption that they lie on top of the Tournaisian-lower Visean limestone unit (Figure 4). This limestone unit has been karstified indicating emergence and weathering, and the karst cavities have been infilled with an upper lower Visean chert-rich unit; these two observations constrain the exposure age. Finally, the trachyandesitic bodies display columnar and planar jointing and vesicular and microlitic texture, which would indicate subaerial emplacement and furthermore, their top surface, like the Tournaisian-lower Visean limestone one, has also been weathered. On the other hand, the $^{40}Ar/^{39}Ar$ ages obtained for these rocks are distinctly different: they vary from 226 (UK07) to 278 Ma (UK06), which is much younger than the stratigraphic age. Since the age spectra display very good plateau ages (Figure 6), their most straightforward and most logical meaning can only be as corresponding to the emplacement ages.

[29] The three dacite units (UK12, UK55, and 37-1) have a chronostratigraphic age of Late Devonian (Frasnian, circa 367 Ma; Figure 4), defined on the basis of their absence in any of the overlying units. They also display columnar and planar jointing and seem to overlie, in some locations, Devonian sediments and lava flows [*McCann et al.*, 2003]. Here again, the $^{40}Ar/^{39}Ar$ ages obtained are different from the chronostratigraphic ones: they all belong to the age group of circa 220 Ma (Late Triassic).

6.2.2. Scythian Platform

[30] The obtained $^{40}Ar/^{39}Ar$ ages are often different from the stratigraphic ones, derived from the position of the units sampled in the stratigraphic sequence (Figure 4). This discrepancy is most evident for the three samples from drill hole Svetloiarskaya 102 (AN4, AN5, and AN6), for which the $^{40}Ar/^{39}Ar$ ages are best defined by pseudoplateau ages or average ages on flat portions of the spectrum (Figure 7). The chronostratigraphic age of these samples was defined as Early to Middle Triassic (~240 Ma); their $^{40}Ar/^{39}Ar$ ages vary between 208 and 179 Ma (Early Jurassic). For two of the samples (AN10 and AN11), the spectra are too disturbed to permit relevant comparison (Figure 7). Finally, the $^{40}Ar/^{39}Ar$ age of sample AN12 (pseudoplateau age of circa 174 Ma) corresponds to that derived from its stratigraphic position.

[31] The observed discrepancies between the $^{40}Ar/^{39}Ar$ and chronostratigraphic ages, both in the Donbas Fold Belt and in the Scythian Platform, have to be explained in order to assess the meaning of the $^{40}Ar/^{39}Ar$ ages obtained. Simplistically, there are two alternatives, as follows:

[32] 1. The relationships between the various sedimentary and igneous units are often problematic, which hampers their correct interpretation and determination of the corresponding stratigraphic ages. Indeed, in some cases, these relationships have been inferred by observation of disconnected outcrops or in drill holes, which may have misled the interpretation in the case of unobserved structural perturbations or of ambiguous contacts.

[33] 2. The $^{40}Ar/^{39}Ar$ ages do not correspond to the emplacement ages of the igneous units as a result of subsequent perturbation and/or resetting of the isotopic systems of the dated minerals. Thermal perturbation can be a consequence of abnormally high heat flow [e.g., *Sachsenhofer et al.*, 2002] or of magmatic activity, as proposed for the age of the plagioclase from sample UK06. However, in most cases, this is certainly not possible, given that the reopening temperature of the dated minerals is quite high (amphiboles: 550° to 650°C) [*Villa*, 1998]; if the massif had been subject to such reheating, observable changes would be present, such as recrystallization, and they are not.

[34] Finally, the possibility of alteration causing perturbation of the argon system of the minerals (argon loss or

Table 2. Analytical Data for the $^{40}Ar/^{39}Ar$ Dating of the Samples From the Donbas Fold Belt and the Scythian Platform[a]

Step	$^{36}Ar/^{40}Ar$	±2σ	$^{39}Ar/^{40}Ar$	±2σ	^{40}Ar Air, %	^{39}Ar, %	$^{40}Ar^*/^{39}Ar_K$	±2σ	Age, Ma	±2σ
Sample UK06, Plagioclase, Plateau Age: 251.4 ± 4.2 Ma										
1	0.000027	0.000021	0.043502	0.000127	0.81	48.8	22.804	0.079	**251.36**	1.63
2	0.000006	0.000045	0.043712	0.000159	0.17	24.1	22.839	0.157	**251.72**	3.24
3	0.000043	0.000102	0.044320	0.000328	1.27	7.5	22.279	0.351	**245.95**	7.24
4	0.000020	0.000124	0.042534	0.000177	0.59	9.0	23.375	0.435	**257.22**	8.92
5	0.000047	0.000196	0.042197	0.000356	1.39	4.5	23.370	0.693	**257.18**	14.21
6	0.000096	0.000202	0.042573	0.000333	2.84	6.1	22.824	0.707	**251.5**7	14.54
Sample UK06, Amphibole, Plateau Age: 278.1 ± 5.3 Ma										
1	0.001432	0.001124	0.033207	0.001282	42.31	1.6	17.373	5.012	194.59	106.44
2	0.000194	0.000109	0.038502	0.000353	5.74	15.1	24.484	0.433	268.56	8.82
3	0.000063	0.000067	0.038847	0.000223	1.87	22.9	25.263	0.265	**276.48**	5.38
4	0.000112	0.000122	0.038622	0.000293	3.33	11.2	25.032	0.478	**274.14**	9.71
5	0.000044	0.000046	0.038618	0.000150	1.30	49.2	25.561	0.182	**279.51**	3.69
Sample N4, Biotite, Plateau Age: 277.7 ± 5.8 Ma										
1	0.002776	0.000475	0.009158	0.000340	82.04	0.7	19.617	7.670	218.27	160.75
2	0.002471	0.000765	0.019822	0.000453	73.02	0.9	13.613	5.705	154.23	123.89
3	0.001451	0.000509	0.027373	0.000367	42.89	2.2	20.864	2.752	231.29	57.27
4	0.000286	0.000320	0.034047	0.000528	8.46	2.8	26.888	1.403	292.90	28.21
5	0.000165	0.000123	0.035825	0.000176	4.88	11.2	26.552	0.512	289.52	10.32
6	0.000106	0.000042	0.037679	0.000196	3.14	22.3	25.708	0.177	**281.00**	3.58
7	0.000093	0.000097	0.038320	0.000256	2.76	13.4	25.378	0.383	**277.66**	7.78
8	0.000048	0.000051	0.038887	0.000170	1.43	25.4	25.349	0.202	**277.36**	4.10
9	0.000119	0.000059	0.038814	0.000159	3.53	19.0	24.856	0.231	**272.35**	4.70
10	0.000000	0.000000	0.038187	0.000919	0.01	1.1	26.187	0.315	285.84	6.36
11	0.000141	0.001793	0.038074	0.000731	4.18	1.2	25.169	6.963	275.54	141.38
Sample UK07, Amphibole, Plateau Age: 226.0 ± 34.7 Ma										
1	0.000711	0.003354	0.031712	0.002524	21.00	4.3	24.913	31.313	272.93	318.36
2	0.000000	0.000000	0.036348	0.010054	0.01	1.3	27.512	7.610	299.16	76.25
3	0.000376	0.002326	0.041868	0.001964	11.13	7.9	21.229	16.447	235.08	170.76
4	0.000096	0.000887	0.047070	0.000864	2.86	22.8	20.639	5.582	**228.95**	58.15
5	0.000073	0.001514	0.048969	0.001227	2.18	13.5	19.978	9.151	**222.05**	95.70
6	0.000056	0.001636	0.047470	0.001409	1.66	12.8	20.718	10.204	**229.77**	106.25
7	0.000133	0.001034	0.047273	0.000881	3.94	20.3	20.322	6.474	**225.64**	67.57
8	0.000156	0.001279	0.047900	0.001074	4.62	17.1	19.915	7.904	**221.39**	82.68
Sample UK12, Amphibole, Plateau Age: 219.3 ± 31.3 Ma										
1	0.000213	0.001547	0.043524	0.008772	6.31	11.1	21.527	5.682	238.18	117.78
2	0.000189	0.000849	0.043737	0.004291	5.60	23.1	21.584	3.058	**238.77**	63.37
3	0.000144	0.000676	0.050507	0.004255	4.28	27.2	18.955	2.134	**211.31**	44.90
4	0.000646	0.004871	0.040680	0.023474	19.09	4.1	19.892	18.604	**221.14**	389.30
5	0.000111	0.001323	0.046916	0.008192	3.30	13.9	20.614	4.539	**228.68**	94.59
6	0.000295	0.001143	0.048849	0.005833	8.71	20.6	18.690	3.634	**208.52**	76.57
Sample UK55, Amphibole, Plateau Age: 214.3 ± 12.7 Ma										
1	0.003199	0.002626	0.024069	0.023412	94.54	0.7	2.268	16.158	26.63	376.61
2	0.002861	0.003263	0.047149	0.013596	84.55	2.5	3.278	10.237	38.36	237.07
3	0.001554	0.001394	0.050738	0.004635	45.92	7.6	10.660	4.088	121.87	90.39
4	0.001356	0.000964	0.048829	0.003846	40.09	8.9	12.271	2.957	139.60	64.73
5	0.000014	0.000297	0.051053	0.001515	0.43	24.8	19.506	0.908	**217.10**	19.04
6	0.000106	0.000956	0.051473	0.003300	3.14	11.5	18.820	2.809	**209.89**	59.15
7	0.000087	0.000532	0.052027	0.002933	2.57	12.3	18.729	1.601	**208.94**	33.74
8	0.000011	0.000322	0.051748	0.001839	0.32	20.4	19.264	0.981	**214.57**	20.60
9	0.000045	0.001254	0.052595	0.011335	1.35	3.3	18.758	4.061	**209.24**	85.55
10	0.000304	0.000951	0.049078	0.004408	8.99	8.0	18.545	2.983	**207.00**	62.92
Sample 37-1, Amphibole, Plateau Age: 214.3 ± 14.2 Ma										
1	0.001132	0.001439	0.043171	0.001866	33.45	4.6	15.416	4.937	173.69	106.07
2	0.000275	0.000575	0.048311	0.000617	8.12	13.0	19.019	1.764	**211.99**	37.10
3	0.000276	0.000404	0.048372	0.000537	8.17	20.7	18.985	1.239	**211.63**	26.07
4	0.000023	0.000404	0.050744	0.000469	0.70	23.6	19.571	1.181	**217.78**	24.75
5	0.000010	0.000628	0.050891	0.000745	0.32	14.9	19.589	1.830	**217.98**	38.36
6	0.000032	0.001158	0.051674	0.000742	0.95	9.4	19.170	3.314	**213.57**	69.63
7	0.000055	0.000729	0.052187	0.000624	1.65	13.7	18.848	2.067	**210.19**	43.52
Sample N2, Amphibole, Plateau Age: 153.1 ± 4.6 Ma										
1	0.002927	0.000628	0.011855	0.001275	86.49	1.0	11.392	7.856	129.94	172.92

Table 2. (continued)

Step	$^{36}Ar/^{40}Ar$	±2σ	$^{39}Ar/^{40}Ar$	±2σ	^{40}Ar Air, %	^{39}Ar, %	$^{40}Ar^*/^{39}Ar_K$	±2σ	Age, Ma	±2σ
2	0.002096	0.001295	0.030319	0.001859	61.95	1.4	12.551	6.323	142.66	138.20
3	0.001212	0.000711	0.052793	0.000831	35.81	5.1	12.159	1.993	**138.37**	43.67
4	0.000801	0.000361	0.061713	0.000634	23.67	12.3	12.370	0.866	**140.67**	18.96
5	0.000292	0.000391	0.067614	0.000966	8.64	14.6	13.513	0.860	**153.14**	18.68
6	0.000178	0.000087	0.069777	0.000324	5.27	65.6	13.578	0.186	**153.85**	4.05
					Sample UK39c, Biotite, Plateau Age: 151.4 ± 4.7 Ma					
1	0.000076	0.013173	0.063723	0.005374	2.26	5.0	15.339	30.550	172.87	656.62
2	0.000411	0.000324	0.066948	0.002003	12.15	14.9	13.123	0.747	**148.90**	16.27
3	0.000915	0.001557	0.063195	0.011791	27.04	2.3	11.546	3.892	**131.64**	85.58
4	0.000021	0.000485	0.068375	0.002838	0.63	10.8	14.535	1.090	**164.21**	23.54
5	0.000811	0.000804	0.068555	0.003496	23.98	8.9	11.090	1.767	**126.62**	38.97
6	0.000180	0.000087	0.070864	0.000721	5.33	58.1	13.361	0.194	**151.49**	4.23
					Sample 34-3, Biotite, Plateau Age: 155.4 ± 3.9 Ma					
1	0.000678	0.000916	0.114402	0.001399	20.06	3.9	6.989	1.184	80.82	26.78
2	0.000007	0.000112	0.076313	0.000474	0.22	11.6	13.077	0.220	148.39	4.79
3	0.000088	0.000320	0.070414	0.000717	2.60	6.7	13.834	0.674	**156.62**	14.63
4	0.000202	0.000329	0.070081	0.000916	5.98	3.5	13.418	0.698	**152.11**	15.18
5	0.000021	0.000335	0.068763	0.000296	0.62	7.2	14.454	0.720	**163.33**	15.56
6	0.000188	0.000208	0.070445	0.000314	5.57	10.9	13.406	0.438	**151.98**	9.52
7	0.000083	0.000125	0.069534	0.000285	2.46	17.4	14.029	0.268	**158.74**	5.80
8	0.000047	0.000109	0.072631	0.000413	1.41	20.0	13.575	0.225	**153.82**	4.90
9	0.000068	0.000151	0.071843	0.000447	2.02	18.8	13.640	0.313	**154.52**	6.79
					Sample AN94-4, Whole Rock, Plateau Age: 204.7 ± 2.1 Ma					
1	0.000480	0.000054	0.064384	0.000328	14.21	11.9	13.327	0.129	130.25	2.42
2	0.000040	0.000016	0.051226	0.000102	1.19	31.1	19.290	0.050	185.63	0.92
3	0.000023	0.000028	0.045929	0.000168	0.70	16.0	21.622	0.099	**206.83**	1.78
4	0.000075	0.000041	0.046713	0.000237	2.21	11.0	20.936	0.141	**200.61**	2.56
5	0.000104	0.000032	0.045395	0.000186	3.09	13.7	21.349	0.113	**204.36**	2.05
6	0.000096	0.000087	0.045649	0.000468	2.83	5.0	21.288	0.303	**203.80**	5.49
7	0.000132	0.000064	0.044619	0.000343	3.90	6.7	21.540	0.227	**206.08**	4.10
8	0.000228	0.000141	0.043684	0.000748	6.73	3.0	21.352	0.513	**204.38**	9.28
9	0.000431	0.000407	0.041943	0.002129	12.75	1.0	20.803	1.535	**199.41**	27.87
10	0.000653	0.000620	0.040117	0.003208	19.29	0.6	20.121	2.434	**193.20**	44.33
					Sample AN94-5, Whole Rock, Plateau Age: 192.9 ± 1.1 Ma					
1	0.000616	0.000005	0.039191	0.000080	16.65	11.3	20.872	0.028	204.91	0.52
2	0.000410	0.000005	0.041958	0.000052	36.18	8.6	20.943	0.022	205.57	0.41
3	0.000371	0.000006	0.041346	0.000042	38.09	8.1	21.535	0.023	211.06	0.42
4	0.000357	0.000006	0.041284	0.000083	14.00	11.2	21.669	0.032	212.29	0.58
5	0.000346	0.000007	0.042296	0.000050	27.75	9.6	21.229	0.027	208.22	0.50
6	0.000367	0.000005	0.043686	0.000068	29.57	9.8	20.407	0.024	200.59	0.44
7	0.000594	0.000008	0.042986	0.000032	51.98	7.1	19.181	0.027	189.15	0.50
8	0.000630	0.000009	0.041479	0.000066	45.95	7.8	19.620	0.035	**193.25**	0.65
9	0.000605	0.000013	0.041962	0.000114	87.08	1.9	19.572	0.053	**192.81**	0.98
10	0.000612	0.000007	0.041870	0.000053	68.82	4.5	19.563	0.029	**192.73**	0.55
11	0.000658	0.000007	0.041176	0.000049	0.00	19.9	19.562	0.028	**192.71**	0.52
					Sample AN94-6, Whole Rock, No Plateau Age					
1	0.001124	0.000015	0.035158	0.000070	33.21	6.5	18.998	0.065	186.23	1.21
2	0.000665	0.000008	0.040108	0.000042	19.66	24.0	20.032	0.030	195.83	0.55
3	0.000353	0.000007	0.043251	0.000054	10.43	9.4	20.709	0.028	202.10	0.51
4	0.000411	0.000007	0.045445	0.000047	12.15	6.7	19.331	0.025	189.33	0.47
5	0.000511	0.000010	0.047114	0.000062	15.11	4.7	18.019	0.034	177.09	0.64
6	0.000729	0.000010	0.042969	0.000047	21.53	10.1	18.262	0.035	179.36	0.65
7	0.000811	0.000008	0.041462	0.000051	23.96	6.1	18.341	0.030	180.10	0.56
8	0.000906	0.000005	0.041454	0.000179	26.77	17.6	17.666	0.043	173.79	0.81
9	0.000834	0.000012	0.041273	0.000048	24.66	5.1	18.255	0.044	179.30	0.82
10	0.000828	0.000009	0.040665	0.000049	24.46	9.7	18.577	0.034	182.30	0.63
					Sample UK07, Amphibole, Plateau Age: 226.0 ± 34.7 Ma					
1	0.000432	0.000005	0.029914	0.000045	12.76	6.4	29.164	0.033	276.12	0.58
2	0.000096	0.000001	0.037593	0.000046	2.84	50.8	25.846	0.016	246.76	0.29
3	0.000057	0.000001	0.039834	0.000027	1.69	26.9	24.682	0.009	236.34	0.16
4	0.000172	0.000005	0.041669	0.000089	5.09	4.4	22.777	0.032	219.17	0.57
5	0.000473	0.000009	0.035461	0.000052	13.99	2.5	24.254	0.040	232.50	0.72
6	0.000447	0.000007	0.036546	0.000055	13.22	1.5	23.745	0.033	227.91	0.60

Table 2. (continued)

Step	$^{36}Ar/^{40}Ar$	±2σ	$^{39}Ar/^{40}Ar$	±2σ	^{40}Ar Air, %	^{39}Ar, %	$^{40}Ar^*/^{39}Ar_K$	±2σ	Age, Ma	±2σ
7	0.000498	0.000004	0.035821	0.000070	14.72	2.2	23.808	0.028	228.48	0.51
8	0.000495	0.000010	0.033664	0.000036	14.64	2.0	25.358	0.044	242.40	0.79
9	0.000604	0.000007	0.031537	0.000046	17.84	1.4	26.053	0.037	248.60	0.65
10	0.000826	0.000011	0.029128	0.000171	24.40	1.3	25.955	0.096	247.73	1.72
11	0.001501	0.000021	0.022082	0.000300	44.35	0.6	25.201	0.225	240.99	4.02
				Sample AN94-11, Whole Rock, No Plateau Age						
1	0.000462	0.000015	0.062511	0.000087	13.65	10.4	13.814	0.037	134.84	0.69
2	0.000255	0.000005	0.069986	0.000077	7.54	58.4	13.213	0.012	129.18	0.23
3	0.000279	0.000006	0.066914	0.000066	8.25	14.9	13.713	0.014	133.89	0.27
4	0.000726	0.000019	0.047543	0.000074	21.46	5.2	16.520	0.060	160.11	1.11
5	0.000851	0.000029	0.039801	0.000102	25.16	1.8	18.805	0.111	181.18	2.04
6	0.000831	0.000015	0.037065	0.000079	24.56	4.0	20.353	0.063	195.32	1.15
7	0.000832	0.000028	0.037279	0.000118	24.58	2.9	20.232	0.116	194.21	2.12
8	0.000779	0.000030	0.041240	0.000062	23.02	2.3	18.666	0.107	179.91	1.96
				Sample AN94-12, Whole Rock, Plateau Age: 174.4 ± 2.1 Ma						
1	0.000150	0.000003	0.118910	0.000105	0.00	12.1	8.038	0.005	78.54	0.10
2	0.000029	0.000160	0.077903	0.000462	59.72	3.0	12.725	0.305	122.82	5.69
3	0.000043	0.000025	0.069757	0.000099	0.00	17.0	14.152	0.054	136.08	1.01
4	0.000023	0.000031	0.061144	0.000101	0.00	12.2	16.244	0.075	155.35	1.38
5	0.000080	0.000010	0.053318	0.000111	0.00	35.6	18.313	0.033	**174.21**	0.59
6	0.000057	0.000057	0.054344	0.000137	0.00	5.8	18.094	0.155	**172.22**	2.82
7	0.000075	0.000061	0.051210	0.000149	0.00	5.1	19.095	0.178	**181.28**	3.22
8	0.000073	0.000131	0.047714	0.000291	52.20	2.2	20.509	0.409	194.01	7.34
9	0.000078	0.000159	0.045866	0.000344	60.54	1.8	21.300	0.518	201.10	9.25
10	0.000071	0.000335	0.045250	0.000718	81.13	0.8	21.634	1.109	204.08	19.78
11	0.000069	0.000214	0.043143	0.000452	70.10	1.3	22.708	0.743	213.63	13.18
12	0.000064	0.000310	0.044859	0.000665	78.79	0.9	21.871	1.034	206.19	18.43
13	0.000045	0.001445	0.045175	0.003085	95.24	0.2	21.843	4.784	205.94	85.24
14	0.000101	0.000163	0.045313	0.000350	57.84	1.9	21.413	0.540	202.11	9.64

[a]Ages of the steps used to calculate a plateau age are indicated in bold.

redistribution) could be invoked, particularly for the Scythian Platform samples where some of the spectra are disturbed as a result of minor alteration. This might be so, but can be excluded where relatively good pseudoplateau $^{40}Ar/^{39}Ar$ ages are observed, such as for samples AN94-4 or AN94-5 (Figure 7).

[35] The $^{40}Ar/^{39}Ar$ ages correspond either to the emplacement of the respective volcanic rock, or to a magmatic event that provoked a total resetting of the argon isotopic system of the dated minerals. In both cases, it is possible to propose that the ages obtained in this work correspond to ages of magmatic activity in the studied areas. Thus it is possible to speak in terms of ages of magmatic activity and to compare them as such.

6.3. Comparison of Ages From the Donbas and the Scythian Platform

[36] All samples from the Donbas Fold Belt provided good plateau ages, while those from the Scythian Platform often produced disturbed age spectra. In order to compare the two sets of ages, it is possible to use the Kernel density analysis technique (Appendix A), based on the ages of all individual steps and their error margins. The use of this technique relies on the hypothesis that the dated phases contain several sites, each of which retains different, but geologically meaningful, age information. For the Scythian Platform samples, which are whole rocks, it is less certain that the age information contained in the individual steps is geologically meaningful, as several phases are probably present. However, the plateaus or pseudoplateaus for the Scythian Platform (Figure 7) have ages very close to those of the peaks observed in the Kernel diagram (Figure 8), which would tend to permit the use of cumulative probability diagrams for these samples and for comparison with samples from the Donbas Fold Belt.

[37] For the Donbas Fold Belt, four peaks are visible in the cumulative probability diagram, corresponding to four ages. Their averages are 153.7 ± 9.7 Ma, 217.1 ± 9.4 Ma, 251.4 ± 4.2 Ma, and 278.8 ± 7.0 Ma (Figure 8). For the Scythian Platform, five peaks are visible, with average ages of 131.2 ± 4.9 Ma, 181.2 ± 2.8 Ma, 193.0 ± 2.1 Ma, 209.2 ± 9.3 Ma, and 243.8 ± 4.7 Ma; one step from sample AN94-10 has an age of 276.1 ± 0.6 Ma (Figure 7). Thus the Early Permian (circa 275 Ma) age group is observed in both areas, as well as the Early Triassic group (circa 245–250 Ma) and the Late Triassic one (circa 205 to 220 Ma; Figure 8). On the other hand, the ages of circa 180 Ma and circa 130 Ma (Middle Jurassic and Early Cretaceous, respectively) from the Scythian Platform are not observed in the Donbas Fold Belt. The validity of the circa 130 Ma age can be questioned as this peak is calculated mostly on low-temperature steps that could probably correspond to isotopically disturbed sites in those samples. Finally, there is one age group in the Donbas Fold Belt (circa 153 Ma, Late Jurassic), which is not observed in the Scythian Platform (Figure 8). Thus it is

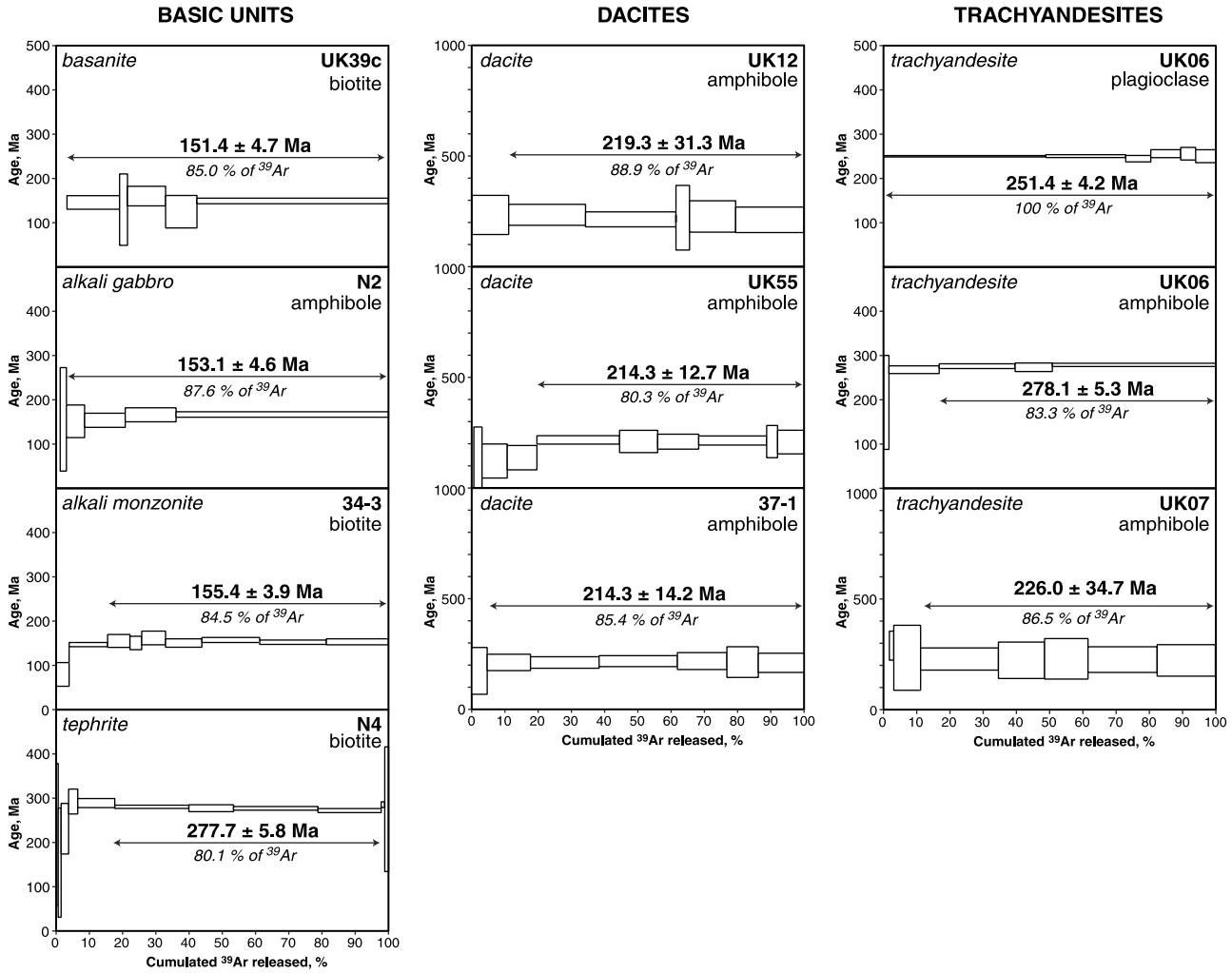

Figure 6. Age spectra for all samples from the Donbas Fold Belt, with the sample name, rock type, mineral, plateau age (in bold), and percentage of gases on which it is calculated (in italics).

possible to say that for the Permian and the Triassic, the timing of magmatic activity in the Donbas and the Scythian Platform are quite similar. For the Jurassic and the Cretaceous, the ages of magmatism in these two areas become different.

6.4. Comparison Between the Ages Obtained and the Ages for the Adjacent Areas

[38] Several authors have proposed ages for the magmatic activity (volcanism) based on the stratigraphy, i.e., chronostratigraphic ages [*Skarzhinsky*, 1973; *Donskoy*, 1982; *Sachsenhofer et al.*, 2002, and references therein]. These syntheses agree in proposing the existence of four major periods of magmatic activity: Late Devonian (Frasnian-Famennian, 380–360 Ma), Early Permian (290–270 Ma), Late Triassic (230–200 Ma), and Late Jurassic-Early Cretaceous (160–110 Ma). Further, the synthesis of many K-Ar ages from the Priazov Massif (south of the Donbas Fold Belt, part of the Ukrainian Shield) [*Shatalov*, 1986, and references therein] reveals the presence of three age groups: Carboniferous-Permian (300–275 Ma), Middle Triassic (240–210 Ma), and Late Jurassic (170–145 Ma).

[39] When the chronostratigraphic ages of the magmatism in the Donbas and the dike ages in the Priazov Massif are compared with the $^{40}Ar/^{39}Ar$ ages obtained in this study from the Donbas Fold Belt and the Scythian Platform (Figure 8), it becomes apparent that (1) the Early Permian magmatic event is present in all the studied areas, and its duration is restricted to the period 285–270 Ma (Figure 8). There is strong similarity in the ages of the Late Triassic magmatic event in the different areas. The duration of this period can be defined as 230 to 200 Ma (Figure 8); (2) the Early Triassic magmatic event (250–245 Ma) is recorded by one plateau age from the Donbas Fold Belt ($UK06_{plagioclase}$) and by ages of individual steps for the Scythian Platform (sample AN94-10), but is not found in the Priazov Massif. It is not indicated by the stratigraphic ages; and (3) there is a strong similarity between the ages of the magmatism in the Donbas and the Scythian Platform until the Jurassic, when these ages become different: the 170 Ma magmatic event in the Scythian Platform is not

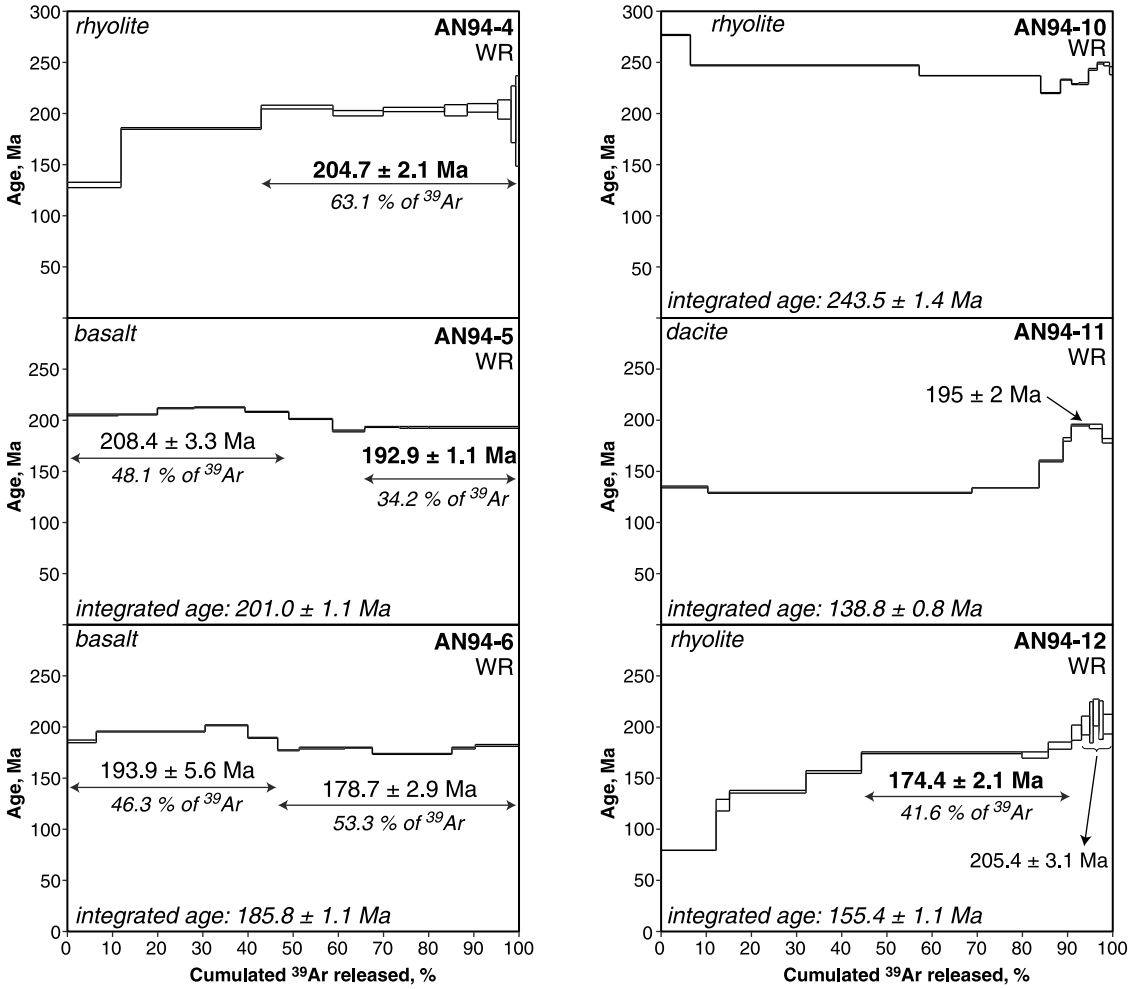

Figure 7. Age spectra for all samples from the Scythian Platform, with the sample name, rock type, mineral, plateau age, and percentage of gases on which it is calculated. Plateau and pseudoplateau ages are given in bold. Average ages over a relatively flat portion on the spectrum are given in regular font; for those samples, the integrated age is given.

apparent in the Donbas, while the circa 150 Ma event from the Donbas is not recorded in the Scythian Platform (Figure 8).

6.5. Significance of the Ages Obtained

[40] The ages in the present work, as well as literature data, indicate that bimodal magmatic activity, expressed in the stratigraphic record by a significant amount of volcanic rocks, was simultaneous in distinct geographic areas, such as the Scythian Platform, the Donbas Fold Belt, and the Priazov Massif, during the Early Permian (285–270 Ma) and the Late Triassic (230–200 Ma), with a minor magmatic event during Early Triassic (245–250 Ma; Figure 8). These three distinct areas represent different geotectonic contexts: a plate (Scythian Platform), an ancient shield (Priazov Massif), and an inverted rift structure (Donbas Fold Belt), which would indicate that the age of magmatism was independent of the geotectonic context. Therefore the source of magmatism itself should be independent of the geodynamic context, which can be achieved if this source were a long-lived and intermittently active mantle plume. This is in agreement with the conclusions of *Chekunov et al.* [1992] and *Wilson and Lyashkevich* [1996], who indicate a deep plume source for the Late Devonian synrift magmatism in the Prypiat-Dnieper-Donets basin, and of *Nikishin et al.* [2002], who indicate the presence of Permo-Triassic short-lived mantle plumes in eastern Europe.

[41] Plumes of similar size (more than 1000 km) have been described in other areas, e.g., Iceland [*O'Connor et al.*, 2000], Trinidade, Brazil [*Gibson et al.*, 1997], Galapagos [*White et al.*, 1993]. The activity of the proposed plume would have lasted at least 80 to 100 Ma (Early Permian to Late Triassic), and have been active at particular periods (every circa 40 Ma), which is similar to the pulsing nature of the Iceland plume observed by *O'Connor et al.* [2000].

[42] Alternative interpretations of the similarity of the magmatism ages in areas with different geodynamic context could be found in the general evolution of this part of the East European Craton (EEC). Its southern margin can be considered an active (Pacific-type) continental margin

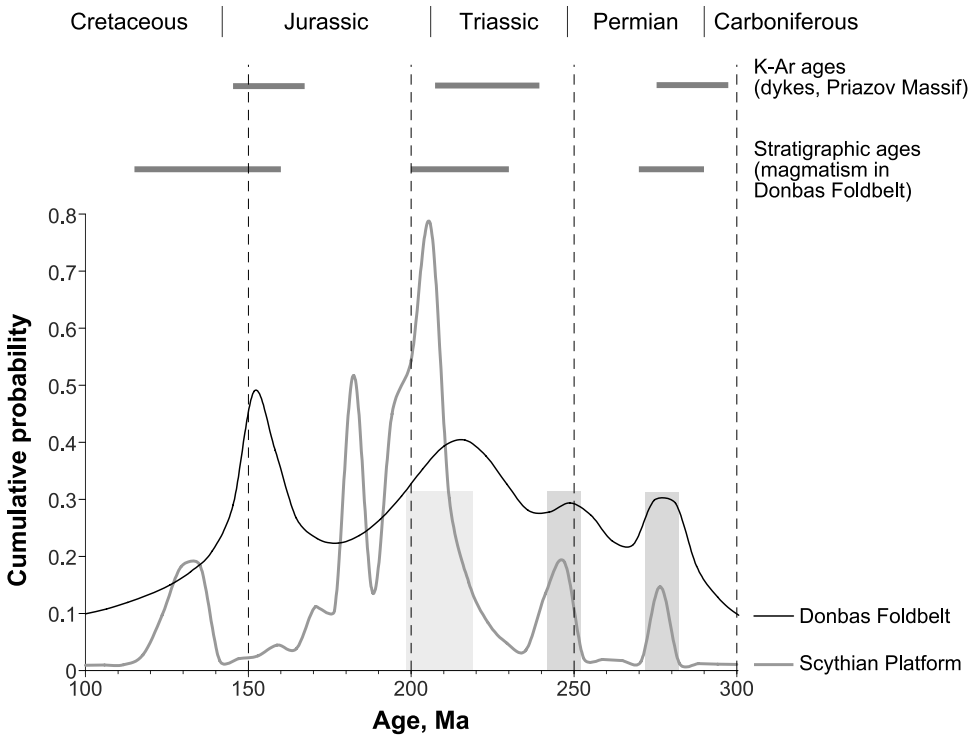

Figure 8. Cumulative probability diagram for the ages of magmatism in the Donbas Fold Belt and the Scythian Platform. The K-Ar ages for dikes in the Priazov Massif [*Shatalov*, 1986, and references therein] and the stratigraphic ages for the magmatism in the Donbas [*Skarzhinsky*, 1973; *Donskoy*, 1982; *Sachsenhofer et al.*, 2002, and references therein] are given for comparison. The shaded bands indicate the ages common to the two areas.

in late Palaeozoic-early Mesozoic times [*Ustaomer and Robertson*, 1994; *Nikishin et al.*, 2001]. In response to north dipping subduction of the Paleo-Tethys area in the Triassic, the Scythian Platform would have been affected by tensional stresses, resulting in the opening of marginal rift and back arc basins. The phase of active extension in the Scythian Platform during the Early-Middle Triassic, probably related to a back arc rifting [*Robinson*, 1997; *Nikishin et al.*, 2001], can be paralleled in the Donbas by the extensional rejuvenation in Early Permian times associated with major uplift of the southern shoulder of the Priazov Massif [*Stovba and Stephenson*, 1999]. The ages of magmatic activity, as obtained in this work and in the available literature (245–250 Ma and 285–270 Ma, respectively), could correspond to these extensional contexts. Further, the Late Triassic-Early Jurassic magmatic activity could correspond to compressional events observed in both the Scythian Platform and the Donbas Fold Belt [*Nikishin et al.*, 1996; *Stovba and Stephenson*, 1999]. Finally, the Early Permian regional uplift, which is well observed in the EEC, can be related to a mantle plume, but can also be a syncompressional orogenic uplift related to an orogenic phase along the Caucasus Belt [*Nikishin et al.*, 1996].

7. Conclusions

[43] Our study brings some new constraints on the evolution of the southern edge of the Eastern European Craton (EEC), which is still a matter of debate. The three synchronous, mainly effusive, magmatic events of Early Permian (285–270 Ma), Early Triassic (250–245 Ma) and Late Triassic (230–200 Ma) age are recorded in a widespread area and occurred in distinct tectonic settings, i.e., the Donbas Rift, the Precambrian Priazov Massif (part of the Ukrainian Shield) and the Scythian Platform; the Early Triassic magmatic event appears to be a minor one. This is consistent with the existence of a mantle plume triggering magmatic activity whatever the tectonic context and the state of the lithosphere (see discussion on mantle plumes and mantle dynamics by *Nikishin et al.* [2002]). Other interpretations of the similar ages can be proposed in the general tectonic evolution of the area, with phases of extension and compression related to an active margin context for the south margin of the EEC, and marked by enhanced magmatism, particularly for the Jurassic and Cretaceous magmatic activity phases. These differing interpretations allow us to consider the geodynamic setting of the southern margin of the EEC as not yet fully determined, and that future work ought to be done. For instance, hydrogen isotopes analyses of the volcanic and superficially intrusive rocks from the various areas would allow one to confirm or infirm the mantle plume hypothesis.

Appendix A: Kernel Density Analysis

[44] The density analysis of a population can be performed using various methods, the most widely used being the

histogram, i.e., the number of samples per segment (''bin'') plotted versus the value measured. This method has two severe limitations: (1) it does not permit the integration of the error on the measures in the calculation of the density and (2) it requires a relatively large number of samples in order to yield meaningful information in terms of group distribution.

[45] A much more pertinent statistical treatment, particularly in the case of lower number of samples, is Kernel analysis, also known as a cumulative probability diagram. This analysis presents several advantages, not the least of which is that it incorporates individual error margins for every data point. The basis of this analysis is the cumulating of the individual probabilities (P_I) for every individual measure at different value of the variable (A). In the case of definition of age groups, where the variable is the age, the formula used is

$$P_I(A) = \frac{\exp -\{(A-M)/\sigma\}^2}{2\pi\sqrt{\sigma}},$$

where A is the age for which the probability, P is calculated, M is the $^{40}Ar/^{39}Ar$ age obtained, and σ is its error margin. The final diagram is obtained by adding the individual probabilities P_I for different values of A:

$$P(A) = \sum P_I(A).$$

Note that the simple Gaussian (normal) distribution formula is used here, given that the error margin is symmetric.

[46] **Acknowledgments.** The authors would like to thank Pavel Fokin (Moscow State University, Russia), who performed part of the $^{40}Ar/^{39}Ar$ analyses, Vitaliy Privalov (Donetsk State Technical University, Ukraine) for fieldwork assistance, Russell Horne (Leeds University, UK) for the petrographic study of the Scythian Platform samples, Arjan Brem (Vrije Universiteit, Netherlands), Anatoly Nikishin (Moscow State University, Russia), and Mykolai Zhykaliak (Donetsk Geological Exploration State Enterprise, Ukraine) for help with samples, as well as all members of Intas/Europrobe Georift Project team who participated in field work and contributed to the advancement of this study. This work took place in the framework of the European Science Foundation Europrobe program and was in part financially supported by the INTAS project 97-0743. The thorough and constructive reviews by P. Fokin, P. Tikhomirov, and an anonymous reviewer greatly improved the quality of the manuscript.

References

Alekseev, A. S., L. I. Kononova, and A. M. Nikishin (1996), The Devonian and Carboniferous of the Moscow Syneclise (Russian Platform): Stratigraphy and sea-level changes, *Tectonophysics*, *268*, 149–168.

Chekunov, A. V., V. K. Gavrish, R. I. Kutas, and L. I. Ryabchun (1992), Dnieper-Donets palaeorift, *Tectonophysics*, *208*, 257–272.

Chekunov, A. V., L. T. Kaluzhnaya, and L. I. Ryabchun (1993), The Dniepr-Donets paleorift, Ukraine, deep structures and hydrocarbon accumulations, *J. Pet. Geol.*, *16*, 183–196.

De Boorder, H., A. J. J. van Beek, A. H. Dijkstra, L. S. Galetsky, G. Koldewe, and B. S. Panov (1996), Crustal architecture of the Donets Basin, tectonic implications for diamond and mercury-antimony mineralization, *Tectonophysics*, *268*, 293–309.

Donskoy, A. N. (1982), *Nephelinic Complex of Oktyabrsky Alkaline Massif* (in Russian), 151 pp., Naukova Dumka, Kiev, Ukraine.

Gibson, S. A., R. N. Thompson, R. K. Weska, A. P. Dickin, and O. H. Leonardos (1997), Late Cretaceous rift-related upwelling and melting of the Trinidade starting mantle plume head beneath western Brazil, *Contrib. Mineral. Petrol.*, *126*, 303–314.

Koppers, A. A. P. (2002), ArArCALC—Software for $^{40}Ar/^{39}Ar$ age calculations, *Comput. Geosci.*, *28*(5), 605–619.

Kusznir, N. I., A. Kovkhuto, and R. A. Stephenson (1996a), Syn-rift evolution of the Pripyat Trough, constraints from structural and stratigraphic modeling, *Tectonophysics*, *268*, 221–236.

Kusznir, N. I., S. Stovba, R. A. Stephenson, and K. N. Poplavsky (1996b), The formation of the N. W. Dniepr-Donets Basin, 2D forward and reverse syn-rift and post-rift modeling, *Tectonophysics*, *268*, 237–255.

McCann, T., A. Saintot, F. Chalot-Prat, A. Kitchka, P. Fokin, A. Alekseev, and the EUROPROBE-INTAS Research Team (2003), Evolution of the southern margin of the Donbas (Ukraine) from Devonian to Early Carboniferous times, in *Tracing Tectonic Deformation Using The Sedimentary Record*, edited by T. McCann and A. Saintot, *Geol. Soc. Spec. Publ.*, *208*, 117–135.

McDougall, M., and T. M. Harrison (1999), *Geochronology and Thermochronology by the $^{39}Ar/^{40}Ar$ Method*, Oxford Univ. Press, New York.

Nikishin, A. M., et al. (1996), Late Precambrian to Triassic history of the East European Craton: Dynamics of sedimentary basin evolution, *Tectonophysics*, *268*, 23–63.

Nikishin, A. M., P. A. Ziegler, D. I. Panov, B. P. Nazarevich, M.-F. Brunet, R. A. Stephenson, S. N. Bolotov, M. V. Korotaev, and P. L. Tikhomirov (2001), Mesozoic and Cenozoic evolution of the Scythian Platform-Black Sea-Caucasus domain, in *Peri-Tethys Memoir 6: Peri-Tethyan Rift/Wrench Basins and Passive Margins*, edited by P. A. Ziegler et al., *Mem. Mus. Natl. Hist. Nat.*, *186*, 295–346.

Nikishin, A. M., P. A. Ziegler, D. Abbott, M.-F. Brunet, and S. Cloetingh (2002), Permo-Triassic intraplate magmatism and rifting in Eurasia: Implications for mantle plumes and mantle dynamics, *Tectonophysics*, *351*, 3–39.

O'Connor, J. M., P. Stoffers, J. R. Wijbrans, P. M. Shannon, and T. Morrissey (2000), Evidence from episodic seamount volcanism for pulsing of the Iceland plume in the past 70 Myr, *Nature*, *408*, 954–957.

Renne, P. R., C. C. Swisher, A. L. Deino, D. B. Karner, T. L. Owens, and D. J. DePaolo (1998), Intercalibration of standards, absolute ages and uncertainties in $^{40}Ar/^{39}Ar$ dating, *Chem. Geol.*, *145*, 117–152.

Robinson, A. G. (Ed.) (1997), Regional and petroleum geology of the Black Sea and surrounding regions, *AAPG Mem.*, *68*, 385 pp.

Sachsenhofer, R. F., V. A. Privalov, M. V. Zhykalyak, C. Bueker, E. A. Panova, T. Rainer, V. A. Shymanovskyy, and R. Stephenson (2002), The Donets Basin (Ukraine/Russia): Coalification and thermal history, *Int. J. Coal Geol.*, *49*, 33–55.

Saintot, A., R. Stephenson, A. Brem, S. Stovba, and V. Privalov (2003a), Paleostress field reconstruction and revised tectonic history of the Donbas fold and thrust belt (Ukraine and Russia), *Tectonics*, *22*(5), 1059, doi:10.1029/2002TC001366.

Saintot, A., R. Stephenson, S. Stovba, and Y. Maystrenko (2003b), Structures associated with inversion of the Donbas Foldbelt (Ukraine and Russia), *Tectonophysics*, *373*, 181–207.

Shatalov, N. N. (1986), Dykes of the Priazovie (in Russian), IGS publication, 192 pp., Naukova Dumka, Kiev, Ukraine.

Shchipansky, A. A., and S. V. Bogdanova (1996), The Sarmatian crustal segment: Precambrian correlation between the Voronezh Massif and the Ukrainian Shield across the Dniepr-Donets Aulacogen, *Tectonophysics*, *268*, 109–125.

Skarzhinsky, V. I. (1973), *Endogenous Metallogeny of the Donets Basin* (in Russian), 204 pp., Naukova Dumka, Kiev, Ukraine.

Stephenson, R. A., and Europrobe Intraplate Tectonics and Basin Dynamics Dnieper-Donets and Polish Trough Working Groups (1993), Continental rift development in Precambrian and Phanerozoic Europe: Europrobe and the Dnieper-Donets Rift and Polish Trough basins, *Sediment. Geol.*, *86*, 159–175.

Stovba, S. M., and R. A. Stephenson (1999), The Donbass Foldbelt: Its relationships with the uninverted Donets segment of the Dniepr-Donets Basin, Ukraine, *Tectonophysics*, *313*, 59–83.

Stovba, S. M., R. A. Stephenson, and M. Kivshik (1996), Structural features and evolution of the Dnieper-Donets Basin, Ukraine, from regional seismic reflection profiles, *Tectonophysics*, *268*, 127–147.

Stovba, S. M., Y. P. Maystrenko, R. A. Stephenson, and N. J. Kusznir (2003), The formation of the southeastern part of the Dniepr-Donets Basin: 2-D forward and reverse syn-rift and post-rift modeling, *Sediment. Geol.*, *156*, 11–33.

Ustaomer, T., and A. H. F. Robertson (1994), Late Palaeozoic marginal basin and subduction-accretion: Evidence from the Palaeotethyan Küre Complex, Central Pontides, northern Turkey, *J. Geol. Soc. London*, *151*(2), 291–305.

Villa, I. (1998), Isotopic closure, *Terra Nova*, *10*, 42–47.

White, W. M., A. R. McBirney, and R. A. Doncan (1993), Petrology and geochemistry of the Galapagos Islands: Portrait of a pathological mantle plume, *J. Geophys. Res.*, *98*, 19,533–19,563.

Wilson, M., and Z. M. Lyashkevich (1996), Magmatism and the geodynamics of rifting of the Pripyat-Dnieper-Donets rift, East European Platform, *Tectonophysics*, *268*, 65–81.

Ziegler, P. A. (1990), *Geological Atlas of Western and Central Europe*, 2nd ed., 239 pp., Geol. Soc., Bath, UK.

P. Alexandre, Department of Geological Sciences, Queen's University, Kingston Ontario, Canada K7L 3N6. (pavel@geol.queensu.ca)

F. Chalot-Prat, CRPG-CNRS, B.P. 20, F-54501 Vandoeuvre-les-Nancy, France.

A. Kitchka, CASRE, Suite 429, 55b Gonchar Street, Kiev 01601, Ukraine.

A. Saintot, R. Stephenson, and J. Wijbrans, Faculteit der Aard en Levenswetenschappen, Tektoniek afdeling, Vrije Universiteit, De Boelelaan 1085-1087, NL-1081 HV Amsterdam, Netherlands.

S. Stovba, Technology Centre, Ukrgeofisika, 10, S. Perovska, Kiev 03057, Ukraine.

M. Wilson, School of Earth Sciences, University of Leeds, Leeds LS2 9JT, UK.